VOL. 14, NO. 3, FEBRUARY2019 ISSN 1819-6608
ARPN Journal of Engineering and Applied Sciences

www.arpnjournals.com

HYDROTHERMAL SYNTHESIS OF NANO BST ALLOY AND STUDYING THE PIEZOELECTRIC, OPTICAL PROPERTIES OF POLY (VINYLIDENEFLUORIDE) (PVDF)/$Ba_{0.6}Sr_{0.4}TiO_3$ (BST) NANOCOMPOSITES

Aws K. Mohammed[1], Farah T. M. Noori[2] and Sabah A. Salman[1]
[1]Department of Physics, University of Diyala, College of Science, Diyala, Iraq
[2]Department of Physics, University of Baghdad, College of Science, Baghdad, Iraq
E-Mail: pro.dr_sabahanwer@yahoo.com

ABSTRACT

Ceramic-polymer nanocomposites, consisting of Barium Strontium Titanate (BST) as fillers and Poly(vinylidenefluoride) (PVDF) as matrix, have been fabricated by using a solution casting method with (BST) filler contents of (25–40) vol%. (BST) nanopowder was synthesized by hydrothermal method. The dielectric and optical properties of (PVDF/BST) nanocomposites have been investigated. The (XRD) results showed that the (BST) nanopowder obtained by hydrothermal method with a perovskite structure. The frequency dependency of dielectric constant and dielectric losses of the (PVDF/BST) naocomposites with different volume fractions of (BST) filler in frequency range (50Hz–5MHz) at room temperature were studied. The dielectric constant of the (PVDF/BST) nanocomposites increased with the increasing of (BST) filler. The dielectric losses of the (PVDF/BST) nanocomposites increase with BST filler increasing at the same frequency. The dielectric properties of (PVDF) were improved by increasing (BST) filler. The optical properties were studied from the absorbance spectrum, the absorbance of the (PVDF/BST) nanocomposites increase with the increasing of (BST) filler content. The optical energy gap for the direct allowed electronic transition of (PVDF/BST) nanocomposite with different filler contents of (BST) decreases from (3.7 eV) to (3.2 eV) with the increasing of the (BST) filler content. The results of piezoelectric measurements showed that the resistance of all the (PVDF/BST) nanocomposites decreases as the applied pressure increases, the resistance of the (PVDF/$Ba_{0.6}Sr_{0.4}TiO_3$) nanocomposite increased with the increasing of (BST) filler content at the same applied pressure.

Keywords: PVDF/BST Nanocomposites, optical properties, dielectric properties, piezoelectric properties.

INTRODUCTION

Recently, material scientists are putting lots of interest for the development of new multifunctional ceramic, polymer, polymer composite materials for many applications in electronic devices, biodevices and optoelectronic industry. Polymer-ceramic composites have received a significant attention in view of their technological importance in devices such as high energy density capacitors, sensors, actuators, transducers etc. In the context of energy storage device, ferroelectric ceramic polymer composites have been studied world-wide [1-3]. High dielectric constant ferroelectric ceramics such as Pb(Zr, Ti)O_3 (PZT) and $BaTiO_3$ (BT) have been used as fillers in polymer based composites with high dielectric constant and dielectric breakdown strength. The ceramic fillers used to achieve polymer based composites with high dielectric constant and dielectric breakdown strength are limited to ferroelectric ones [4-6]. Ferroelectric Barium Strontium Titanate (BST) has acquired much attention due to their large dielectric constant, composition dependent Curie temperature, high tunable and ferroelectric properties. It is an interesting material for applications such as multilayer ceramic capacitors, piezoelectric and pyroelectric sensors [7]. Polyvinylidene fluoride (PVDF) is a semi-crystalline polymer having remarkable thermal stability, good chemical resistance and extraordinary pyroelectric and piezoelectric properties among polymers. These properties combined with its high elasticity, relative transparency and ease of processing, make this material suitable for various technological applications [2, 8]. (PVDF) shows a complex structure and it can exhibit five distinct crystalline phases related to different chain conformations, known as (α, β, γ, δ and ε) phases. Thus, the use of (PVDF) as matrix in nanocomposites is one of the key parameters for a wide range of applications. The final properties of these nanocomposites mainly depend on parameters such as filler content, method of preparation and the dispersion of nanoparticles into the polymer matrix [9-11].

In this work, dielectric, optical and piezoelectric properties of Poly(vinylidene fluoride) (PVDF)/$Ba_{0.6}Sr_{0.4}TiO_3$ (BST) nanocomposites were studied. The (BST) nanopowders were synthesized by hydrothermal method. (PVDF/BST) nanocomposites were fabricated by using a solution casting method. The effect of content of the (BST) on the microstructure, dielectric, optical and piezoelectric properties of the nanocomposites were investigated.

Experimental procedures

The $Ba_{0.6}Sr_{0.4}TiO_3$ (BST) nanopowder were synthesized by hydrothermal method by using Barium Hydroxide ($Ba(OH)_2.8H_2O$) (HiMedia Lab., India), Strontium Hydroxide ($Sr(OH)_2.8H_2O$) (E. Merck, Germany) and Titanium Dioxide (TiO_2) (Central Drug House (P) Ltd., India) as raw materials. The raw materials were mixed with NaOH-KOH mixture and stirred for (1 h) by using magnetic stirrer. The final suspension was

transferred to a Teflon vessel of an autoclave, and then placed in a digital temperature controlled oven at (160 °C) for (12 h). The obtained powder were washed (5 times) using distilled water at room temperature and then dried the washed powder in the oven at (80 °C) for (10 h). The final product was $Ba_{0.6}Sr_{0.4}TiO_3$ (BST) nanopowder. The (BST) nanopowder were dispersed in an aqueous solution of H_2O_2 (35%) in a magnetic stirrer at (80°C) for (2 h), then the powder were washed with distilled water and ethanol and then dried in the oven at (80°C) for (6 h).

The Poly(vinylidene fluoride) (PVDF) (3F Co., China) and (BST) nanopowder were mixed in Dimethyl formamide (DMF) solvent with various volume fraction ratio. The mixtures were stirred for (9 h) to form stable suspensions. The composite solution was casted on the glass substrate. The film was kept in oven overnight at (50° C) to evaporate the (DMF) solvent. Finally, the (PVDF/BST) samples were peeled off from the glass substrate. Thickness of the samples was in the range (0.2-0.5) mm measured by digital micrometer.

The X-ray diffraction (XRD-6000, SHIMADZU) are used to study the phase composition of the samples. The (AFM) images by (SPM-AA3000) supplied by Angstrom Advanced Inc. (FESEM) type (MIRA3 model - TE-SCAN, Dey Petronic Co.) was used to image the prepared samples. Fourier-transform infrared spectroscopy (FTIR) was recorded by using a IRAffinity-1 spectrometer (SHIMADZU). In addition, the dielectric properties were measured using LCR-8105G (GW Instek).

RESULTS AND DISCUSSIONS

The XRD pattern of the (BST) nanopowder obtained by hydrothermal method is presented in Figure-1. It was shown that the peaks at 2θ that corresponded to 22.4° (100), 31.8° (110), 39.3° (111), 45.69° (200), 51.3° (210) and 56.7° (211) were assigned to (BST) with a perovskite structure (JCPDS Card No. 34-0411). The intensity of the (110) peak is significantly larger compared to other the peaks. No secondary phases were observed.

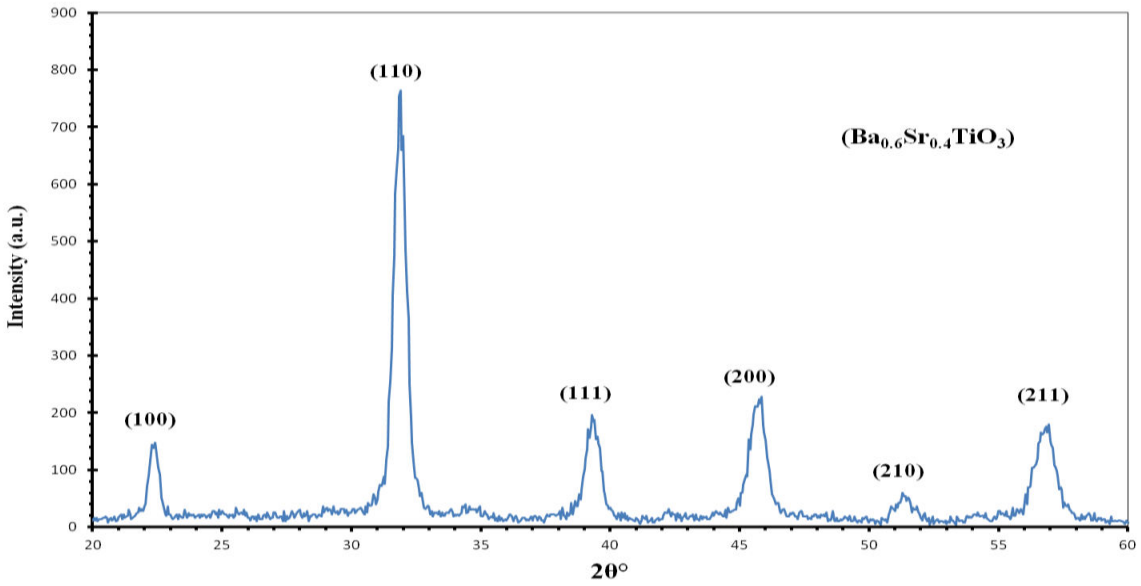

Figure-1. The XRD pattern of BST.

The surface morphology of $Ba_{0.6}Sr_{0.4}TiO_3$ nanopowder synthesized by hydrothermal method was examined by atomic force microscopy (AFM). AFM giving statistics about grain size and its distribution, value of surface roughness depended on root mean square (RMS).

The Figure-2 and explain images of (AFM) for $Ba_{0.6}Sr_{0.4}TiO_3$, (a) is (AFM) picture in three dimensions (3D) and (b) represent particles distribution.

The values of surface topography parameters such as surface roughness is root mean square (RMS) roughness and the grain size for $Ba_{0.6}Sr_{0.4}TiO_3$ nanopowder are summarized in Table-1.

Table-1. (AFM) results of $Ba_{0.6}Sr_{0.4}TiO_3$ nanopowder.

Sample	$Ba_{0.6}Sr_{0.4}TiO_3$
Surface Roughness (nm)	6.01
Root Mean Square Roughness (RMS) (nm)	6.89
Grain Size (nm)	63.28

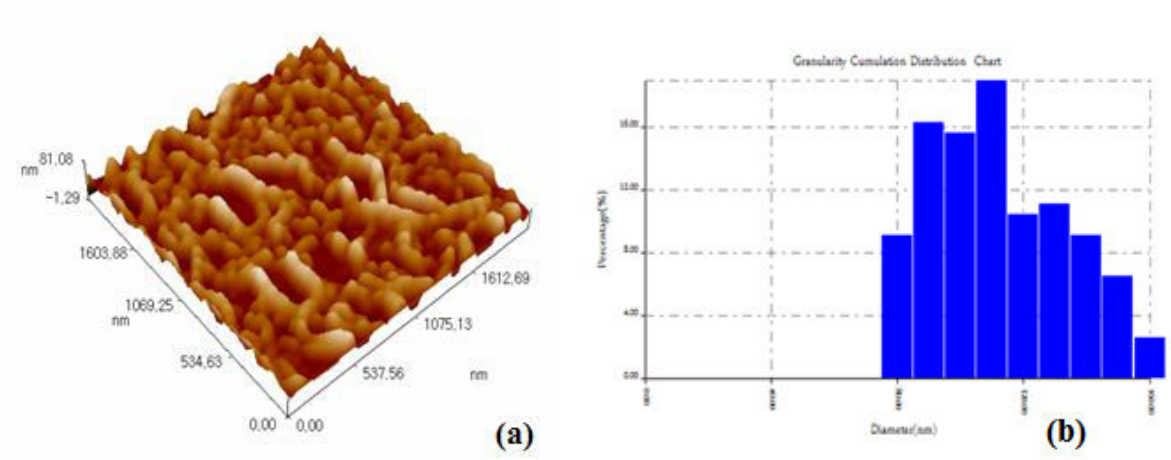

Figure-2. (AFM) of $Ba_{0.6}Sr_{0.4}TiO_3$ nanopowder.

Figure-3 shows (FTIR) spectra of (BST) and BST-OH (after reacting with H_2O_2). The band at (550 cm^{-1}) is associated to the bond vibration of Ti-O [12]. The bands in the region of (1400 cm^{-1}) were attributed to the formation of Ba-O-Ti bond [13]. The new band at (3450 cm^{-1}) of BST-OH corresponded to the stretching mode of -OH [12], confirming the surface hydroxylation of the (BST). When the (BST) particles are mixed with (PVDF) polymer, hydrogen bond will form between the (F atoms) of PVDF molecular chains and the -OH groups on the surface of the BST particles.

Figure-3: (FTIR) spectra of the (BST) and the BST-OH.

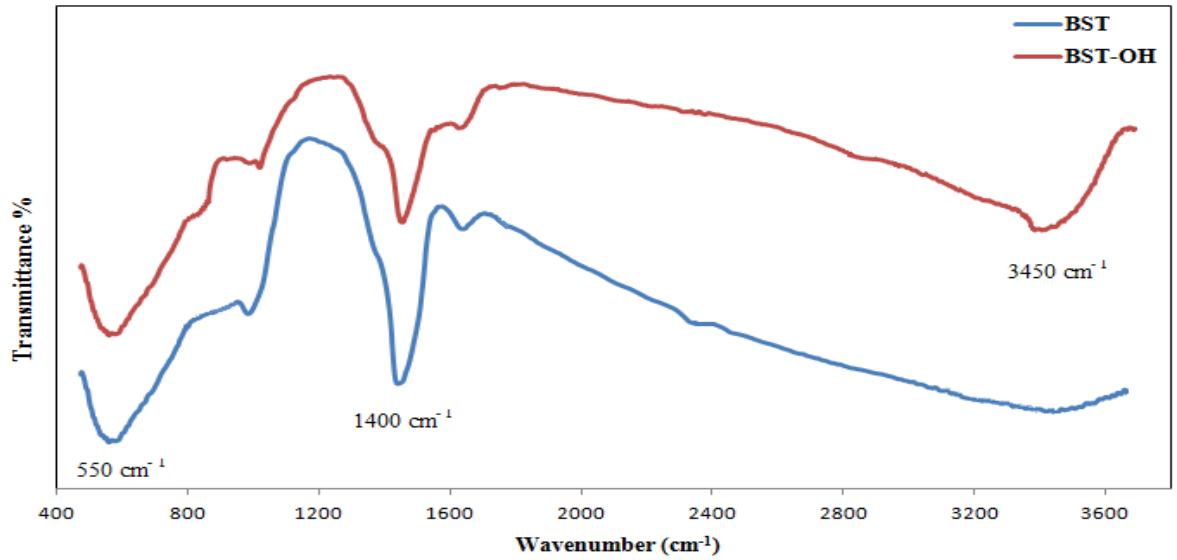

Figure-4. (FTIR) spectra of ($PVDF/Ba_{0.6}Sr_{0.4}TiO_3$) nanocomposites with (25 and 40) vol% filler contents.

It was shown that the bands at (1186 and 2976) cm^{-1} for (α) phase. The bands at (432 cm^{-1}) are of (γ) phase. The bands in the region of (511 and 845) cm^{-1} are attributed to the (β) phase [14, 15]. The band at (1400 cm^{-1}) was attributed to the formation of Ba-O-Ti bond. Each ($PVDF/Ba_{0.6}Sr_{0.4}TiO_3$) nanocomposite exhibits the characteristic absorption bands of (γ, α and β) phases, indicating the (PVDF) polymer matrix are composed of these three phases in the nanocomposites. Moreover, the peak at (1400 cm^{-1}) which is attributed to the formation of Ba-O-Ti bond became stronger with the increase in the content of (BST) filler while those of the (PVDF) polymer phases became quite weak which indicates that the incorporation of (BST) affected the crystalline phase of (PVDF) polymer.

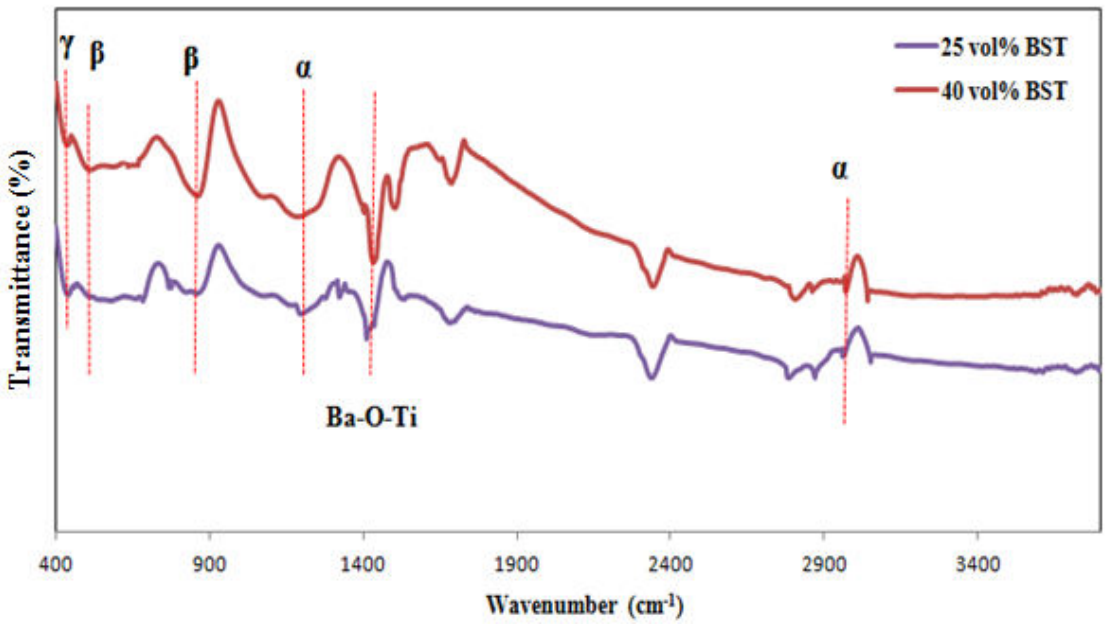

Figure-4. (FTIR) spectra of the (PVDF/BST) composites with different filler contents.

(FESEM) images of (PVDF/$Ba_{0.6}Sr_{0.4}TiO_3$) nanocomposites with (40 vol%) filler content prepared by solution casting method are shown in Figure-5. It is observed that the ceramic particles (BST) are homogenously dispersed in the (PVDF) polymer matrix. From the Figures, The (FESEM) images of the nanocomposites confirm that it contains some pores or voids and vacancies caused by difference in experimental conditions.

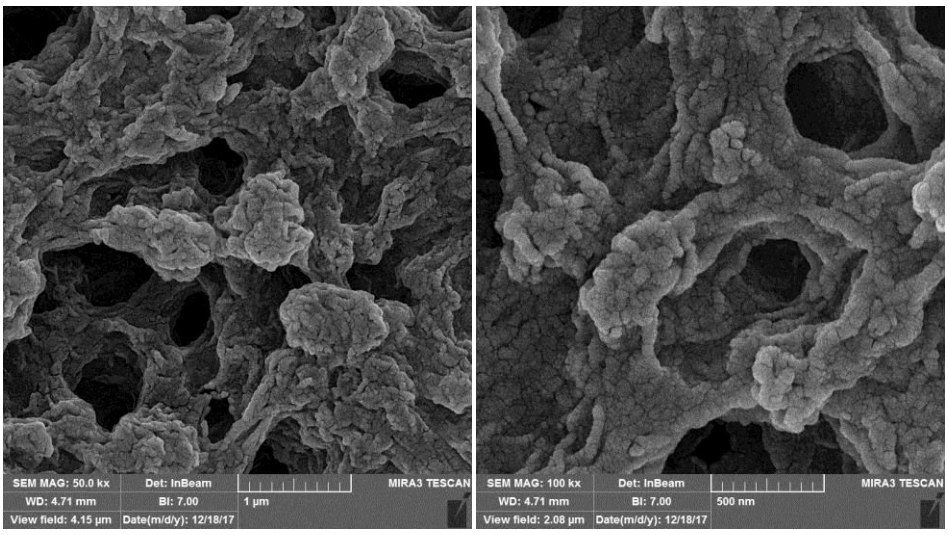

Figure-5. (FESEM) images of (PVDF/BST) nanocomposite with (40 vol%) filler content at different magnifications.

Figure-6 and Figure-7 show the frequency dependency of dielectric constant and dielectric losses of the (PVDF/BST) nanocomposites with (25, 30, 35 and 40) vol% filler contents of (BST) in frequency range (50Hz–5MHz) at room temperature. In Figure 6, one can see that the dielectric constant for the composite (40 vol% BST) has the highest dielectric constant. This confirms that the dielectric constant increases with the increasing of volume fraction of (BST) filler at the same frequency, which should be attributed to the considerably higher dielectric constant of (BST) in comparison with that of the (PVDF). The dielectric constant of all the composites decreases with the increasing of frequency. The phenomenon can be attributed to the polarization relaxation occurring at the inner structure of composites, including interface polarization and dipole orientation polarization [16].

The dielectric losses of (PVDF/BST) composites measured in the frequency range from (50Hz) to (5MHz) at room temperature is shown in Figure-7. The dielectric losses increase slowly with the increasing of volume

fraction of (BST) filler at the same frequency, and the dielectric losses of all the composites decreases with the increasing of frequency.

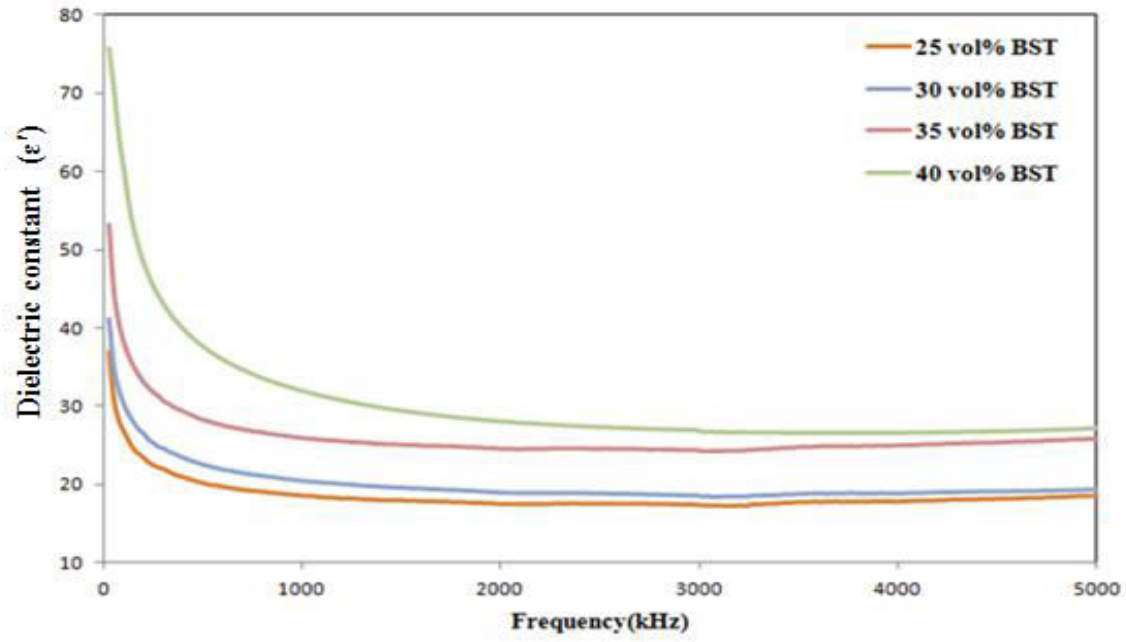

Figure-6. Dielectric constant as a function of frequency of the (PVDF/ BST) composites with different filler contents.

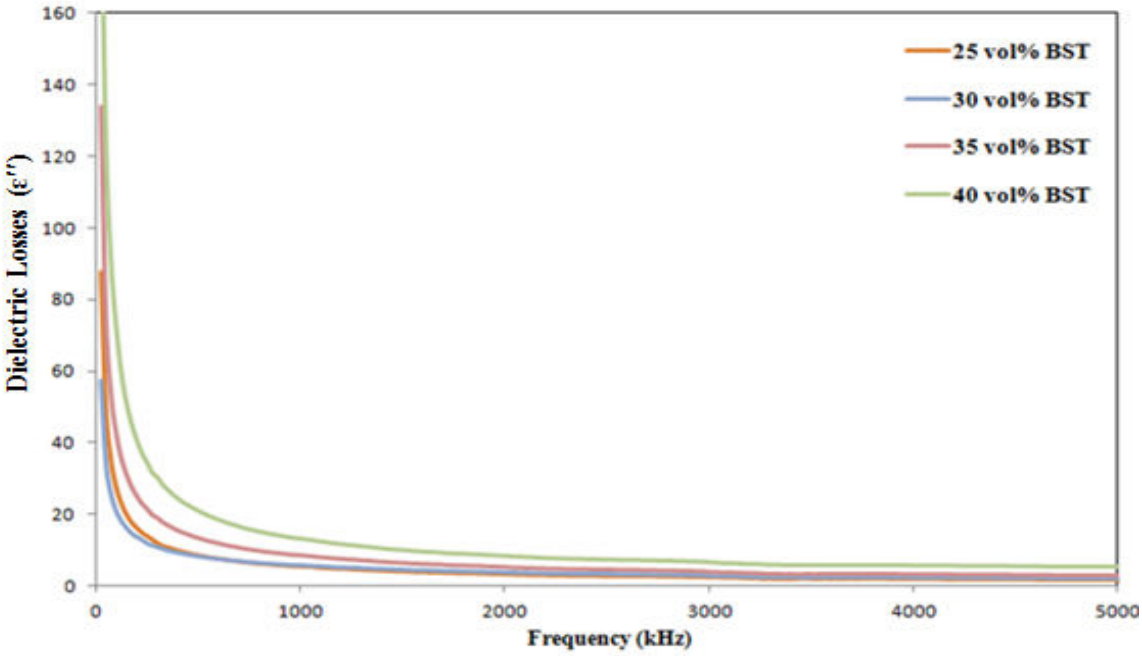

Figure-7. Dielectric losses as a function of frequency of the (PVDF/BST) composites with different filler contents.

Figure-8 shows the relation between absorbance (A) and wavelength (λ) in the range of (300-900) nm for PVDF/ $Ba_{0.6}Sr_{0.4}TiO_3$ (PVDF/BST) nanocomposites solutions with (25, 30, 35 and 40) vol% filler contents. The absorbance of all nanocomposites decreases rapidly at short wavelengths (high energies) corresponding to the energy gap of the material, (when the incident photon has an energy equal or more than the energy gap value). This evident increase of energy is due to the interaction of the material electrons with the incident photons which have enough energy for the occurrence of electron transitions. It

can be observed from the Figure-8 that the absorbance increase with the increasing of volume fraction of (BST).

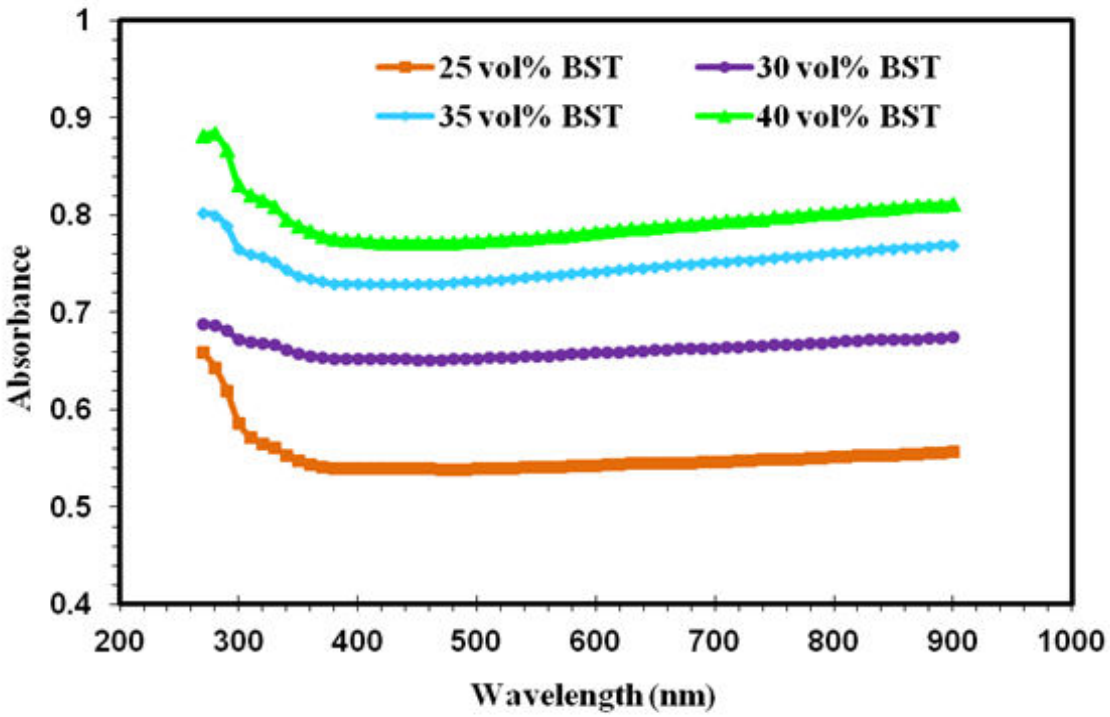

Figure-8. Absorption spectra of (PVDF/BST) nanocomposites with (25, 30, 35 and 40) vol% filler contents.

The optical energy gap for allowed direct transition was calculated by using Tauc's relation [17]:

$$(\alpha h\upsilon = A\left(h\upsilon - E_g\right)^r)$$

where, α is the absorption coefficient, hυ is the photon energy, E_g is the optical band gap, A is constant which depends on the material structure, and the exponent (r=1/2) for allowed direct transition. In this work, direct band gap for (PVDF/BST) nanocomposites with different filler contents was determined by, by plotting a graph between $(\alpha h\upsilon)^2$ and (hυ) in eV, a straight line is obtained from high absorption region. The intercepts (extrapolations) of the straight line to $(\alpha h\upsilon)^2 = 0$ gives value of the optical energy gap of the material, as shown in Figure-9. The optical energy gap for allowed direct transition for (PVDF/BST6) nanocomposites with different filler contents decrease as the (BST6) filler content increases, as shown in Table-2. This behavior may be associated with the structural changes occurring after addition of (BST) filler. Hence the optical energy gap is found to be compositional dependence. This change which indicates a lowering in energy gap leads to an increase in the electrical conductivity of the polymer nanocomposite. This decrease in the optical energy gap value is due to formation of defects and consequently influences the optical properties of materials [18].

Table-2. The optical energy gap for allowed direct transition of (PVDF/BST) nanocomposites with different filler contents.

Sample	25 vol% BST6	30 vol% BST6	35 vol% BST6	40 vol% BST6
Optical Energy Gap (eV)	3.7	3.5	3.4	3.2

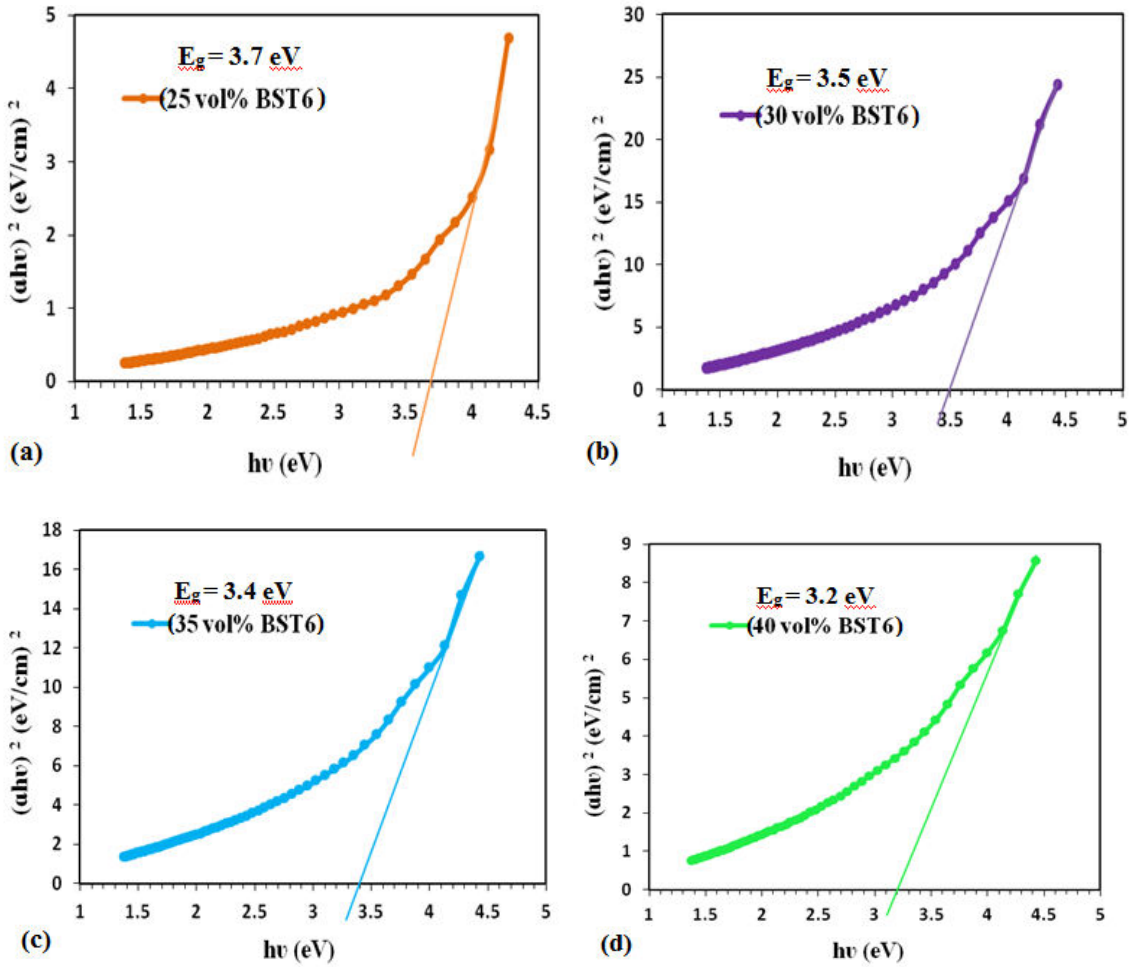

Figure-9. Optical energy gap of (PVDF/BST) nanocomposite with (a) 25 (b) 30 (c) 35 and (d) 40 vol% filler content.

Piezoelectric properties measured by apparatus consists of mechanical press with rang (10 - 7000) bar and ohmmeter (0-250) MΩ.

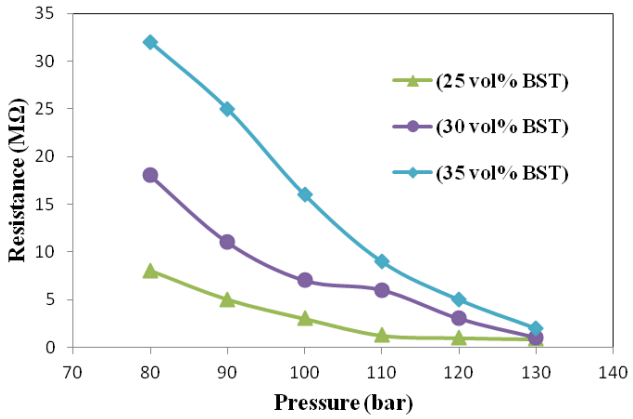

Figure-10. The relation between applied pressure and resistance for (PVDF/BST) nanocomposites with different filler contents.

Mechanical press used to applied stress on a sample between two metal disks. Each disk is encapsulated with insulation material and connects with ohmmeter. Two electrodes were placed between the two disks over the sample, when stress applied on the sample, the ohmmeter measuring the resistance. PVDF/$Ba_{0.6}Sr_{0.4}TiO_3$ (PVDF/BST) nanocomposites films with (25, 30 and 35) vol% filler contents used to examined their piezoelectric effect by applied pressure in the range (80-130) bar and measure the result resistance. Figure-10 shows the relation between applied pressure and resistance for (PVDF/BST) nanocomposites with different filler contents. From the Figure, it can be observed that the resistance of all nanocomposites decreases as the applied pressure increases, this decrease of resistance could be due to the polarization toward the mechanical fields. The resistance of nanocomposite increased with the increasing of (BST) filler content at the same pressure.

CONCLUSIONS

In this study (PVDF/BST) nanocomposites with different filler content were fabricated by using solution casting method. The (XRD) results showed the perovskite structure of (BST) nanopowder. The dielectric constant, dielectric losses of the (PVDF/BST) nanocomposites increase with BST filler increasing at the same frequency. The absorbance of the (PVDF/BST) nanocomposites

increase with the increasing of volume fraction of (BST) filler content. The optical energy gap for the direct allowed electronic transition of (PVDF/BST) nanocomposites with different filler contents of (BST) decrease as the (BST) filler content increases. The results of piezoelectric measurements showed that the resistance of all the (PVDF/BST) nanocomposites decreases as the applied pressure increases, the resistance of the (PVDF/BST) nanocomposite increased with the increasing of (BST) filler content at the same applied pressure.

REFERENCES

[1] S. Abdalla, A. Obaid and F. M. Al-Marzouki. 2016. Preparation and characterization of poly (vinylidene fluoride): A high dielectric performance nano-composite for electrical storage. Results in physics. 6: 617-626.

[2] I. A. Al Ajaj, F. T. Noori and N. N. Ramoo. 2013. Structural and dielectrical study of PZT/PVDF film composites. Int. J. Appl. or Innovation in Eng. Manage. 2(4): 79-88.

[3] K. Yu, H. Wang, Y. Zhou, Y. Bai and Y. Niu. 2013. Enhanced dielectric properties of $BaTiO_3$/poly (vinylidene fluoride) nanocomposites for energy storage applications. Journal of applied physics. 113(3): 034105.

[4] Z. M. Dang, Y. F. Yu, H. P. Xu and J. Bai. 2008. Study on microstructure and dielectric property of the $BaTiO_3$/epoxy resin composites. Composites Science and Technology. 68(1): 171-177.

[5] S. U. Adikary, H. L. W. Chan, C. L. Choy, B. Sundaravel and I. H. Wilson. 2002. Characterisation of proton irradiated Ba0. 65Sr0. 35TiO3/P (VDF-TrFE) ceramic–polymer composites. Composites science and technology. 62(16): 2161-2167.

[6] Y. Bai, Z. Y. Cheng, V. Bharti, H. S. Xu and Q. M. Zhang. 2000. High-dielectric-constant ceramic-powder polymer composites. Applied Physics Letters. 76(25): 3804-3806.

[7] H. V. Alexandru, C. Berbecaru, F.Stanculescu, A. Ioachim, M. G. Banciu, M. I. Toacsen, L. Nedelcu, D. Ghetu and G. Stoica. 2005. Ferroelectric solid solutions (Ba, Sr) TiO3 for microwave applications. Materials Science and Engineering: B. 118(1-3): 92-96.

[8] V. Sencadas, M. V. Moreira, S. Lanceros-Méndez, A. S. Pouzada and R. Gregório Filho. 2006. α-to β Transformation on PVDF films obtained by uniaxial stretch. In Materials science forum. (514): 872-876.

[9] R. G. Kepler and R. A. Anderson. 1978. Piezoelectricity and pyroelectricity in polyvinylidene fluoride. Journal of Applied Physics. 49(8): 4490-4494.

[10] C. K. Chiang and R. Popielarz. 2002. Polymer composites with high dielectric constant. Ferroelectrics. 275(1): 1-9.

[11] H. Ishida S. Campbell and J. Blackwell. 2000. General approach to nanocomposite preparation. Chemistry of Materials. 12(5): 1260-1267.

[12] S. Liu and J. Zhai. 2014. A small loading of surface-modified $Ba_{0.6}Sr_{0.4}TiO_3$ nanofiber-filled nanocomposites with enhanced dielectric constant and energy density. RSC Advances. 4(77): 40973-40979.

[13] A. S. Attar, E. S. Sichani and S. Sharafi. 2017. Structural and dielectric properties of Bi-doped barium strontium titanate nanopowders synthesized by sol-gel method. Journal of materials research and technology. 6(2): 108-115.

[14] P. Martins, A. C. Lopes and S. Lanceros-Mendez. 2014. Electroactive phases of poly (vinylidene fluoride): determination, processing and applications. Progress in polymer science. 39(4): 683-706.

[15] B. Luo, X. Wang, Y. Wang and L. Li. 2014. Fabrication, characterization, properties and theoretical analysis of ceramic/PVDF composite flexible films with high dielectric constant and low dielectric loss. Journal of Materials Chemistry A. 2(2): 510-519.

[16] G. Hu, F. Gao, J. Kong, S. Yang, Q. Zhang, Z. Liu, Y. Zhang and H. Sun. 2015. Preparation and dielectric properties of poly (vinylidene fluoride)/Ba0. 6Sr0. 4TiO3 composites. Journal of Alloys and Compounds. 619: 686-692.

[17] Z. T. Khodair, A. A. Kamil and Y. K. Abdalaah. 2016. Effect of annealing on structural and optical properties of $Ni_{(1-x)}Mn_xO$ nanostructures thin films. Physica B: Condensed Matter. 503: 55-63.

[18] A. P. Indolia and M. S. Gaur. 2013. Optical properties of solution grown PVDF-ZnO nanocomposite thin films. Journal of Polymer Research. 20(1): 43.